

**THREE-PARTICLE PARTIAL AMPLITUDES AND THE UNITARITY CONDITIONS  
FOR COMPLEX VALUES OF THE ANGULAR MOMENTUM**

Ya. I. AZIMOV, A. A. ANSEL'M, V. N. GRIBOV, G. S. DANILOV, and I. T. DYATLOV

A. F. Ioffe Physico-technical Institute, Academy of Sciences, U.S.S.R.

Submitted to JETP editor February 4, 1965

J. Exptl. Theoret. Phys. (U.S.S.R.) 49, 549-571 (August, 1965)

On the basis of some of the simplest Feynman diagrams, we investigate the possibility of analytically continuing the partial amplitudes for the transformation of two particles into three to complex values of the total angular momentum  $j$ . The unitarity conditions with respect to energy of the two produced particles are set up and their properties studied. The properties of the three-particle contribution to the unitarity condition for the scattering amplitude are discussed for complex values of  $j$  in connection with the appearance of Mandelstam branching points.

## INTRODUCTION

THE location and the character of the moving singularities of the partial scattering amplitudes  $f_j(x)$  in the complex plane of the angular momentum  $j$  are determined by the structure of the unitarity condition for  $f_j(x)$  at complex values of  $j$ . As is well known, two-particle intermediate states in the unitarity condition lead to the appearance in the  $j$  plane of only moving poles (Regge poles). Many-particle states can apparently lead also to moving branch points<sup>[1]</sup>.

We have previously considered<sup>[2-3]</sup> a possible mechanism for the occurrence of Mandelstam branch points on the basis of many-particle unitarity conditions for complex  $j$ . The three-particle contribution to the unitarity condition for the partial amplitude was written in<sup>[3]</sup> in the form

$$\Delta f_j(s) = 2 \int d\Gamma_3 \left\{ \sum_{m=0}^{\infty} \frac{\Gamma(j-m+1)}{\Gamma(j+m+1)} f_{jm} f_{j+m}^* + \frac{\pi}{2} \tan \frac{\pi j}{2} \sum_{n=1}^{\infty} \frac{(-1)^{n+1} \varphi_{jj+n} \varphi_{j+j+n}^*}{\Gamma(n) \Gamma(2j+n+1)} \right\}. \quad (1)$$

Here  $f_{jm}$  are the partial amplitudes of the transformation of two particles into three for complex total momentum  $j$  and for integer helicity  $m$ ;  $d\Gamma_3$  is the three-particle phase volume. Let us explain briefly the significance of the appearance of the second term in (1). The unitarity condition (1) has resulted from continuation of the ordinary three-particle unitarity condition, written out for integer  $j$ . Owing to the presence of a signature in  $j$ , the continuation from even and odd values of  $j$  was

carried out separately. Expression (1) corresponds to positive signature. For physical (even)  $j$ , the second term in (1) vanishes, the summation over  $m$  is cut off at  $m = j$ , and the unitarity condition assumes the usual form. Each term of the first sum contains poles in  $j$ , due to the factor  $\Gamma(j-m+1)$ , for all integer  $j < m$ . For even  $j < m$ , however, the positive-signature amplitudes  $f_{jm}$  vanish, and no poles occur in reality. For odd  $j < m$ , the quantities  $f_{jm}$  differ from zero, and since the summation over  $m$  is carried out to infinity, the first sum has poles in  $j$  for all odd  $j$ . These poles are cancelled by the second term in (1)<sup>[3]</sup>. The amplitudes  $\varphi_{jj+n}$  are constructed in this case in the following fashion. The amplitudes  $f_{jm}$  are first continued in  $j$  for fixed integer values of  $m$ . The obtained values of  $f_{jm}$  for odd  $j < m$  serve as the basis for a new continuation in  $j$ , which is carried out at a fixed value of  $m-j = n = 1, 2, \dots$

It was shown earlier<sup>[3]</sup> that the amplitudes  $\varphi_{jj+n}$  for the conversion of two particles into three have a pole in  $j$ , connected with the paired interaction of the produced particles. This pole is located at the point  $j = \alpha(s_{12}) - n$ , where  $\alpha(s_{12})$  is the trajectory of the Regge pole of the interacting pair of particles 1 and 2 ( $\sqrt{s_{12}}$  is the pair energy). After integrating over the phase volume  $d\Gamma_3$  in (1), such poles lead to the appearance of Mandelstam branch points<sup>[2,3]</sup>. We note that it is clear from the method of constructing the quantities  $\varphi_{jj+n}$  that they differ from zero only in the presence of a signature in the amplitudes  $f_{jm}$ . This fact agrees with the results of Mandelstam<sup>[1]</sup>, who has shown that the branch points arise only in certain pertur-

bation-theory diagrams. The latter circumstance will be explained in greater detail in Sec. 4.

The properties of the amplitudes  $f_{jm}$  and  $\varphi_{jj+n}$  with complex  $j$  were not investigated in [3]. In the present paper we investigate the possibility of continuing the partial amplitudes  $f_{jm}$  and  $\varphi_{jj+n}$  to include complex  $j$ , and investigate their properties for the simplest Feynman diagrams. In Sec. 2 we describe a rather general method for analytic continuation of the amplitudes  $f_{jm}$  in  $j$  for fixed integer values of  $m$ . Unlike the continuation of two-particle partial amplitudes, in the case of conversion of two particles into three it is impossible to construct a continuation which decreases in arbitrary direction in the right half-plane of  $j$ . This is connected with the existence of complex singularities in the cosine of the scattering angle. Nonetheless, we can construct a function that increases in the right half plane of  $j$  more slowly than  $\exp(\pi |\operatorname{Im} j|/2)$ . According to the Carleman theorem, the continuation satisfying this requirement is unique.

The concrete character of the asymptotic behavior of  $f_{jm}$  relative to  $j$  depends on the values of the pair energies of the produced particles. Namely, the physical region of the values of the pair energies (circle on the Dalitz diagram, Fig. 6) breaks up into several parts (1, 2, 3, and 4 on Fig. 6), in each of which it is possible to construct uniquely a slowly growing function  $f_{jm}$ . When these functions are continued in the pair energies beyond the limits of the initial region, they become, generally speaking, functions that grow more rapidly than  $\exp(\pi |\operatorname{Im} j|/2)$ . Thus, there exist several continuations of  $f_{jm}$  in  $j$  (at least three), each of which increases slowly only in a definite part of the principal region, and there exists no single continuation that grows slowly in the entire circle and is analytic in the pair energies. The presence of several analytic functions  $f_{jm}$  is analogous to the existence of a signature in the two-particle case, which arises because the contributions of the first and second cuts are continued to complex  $j$  in different fashions. In the three-particle case the number of cuts of the corresponding absorption parts increases (there are at least six of them), and the number of independent functions  $f_{jm}$  increases simultaneously.

In Sec. 3 we consider in explicit form the continuations of  $f_{jm}$  in  $j$  for the simplest Feynman diagrams (Fig. 4). For these diagrams we construct also the quantities  $\varphi_{jj+n}$ , which enter in the unitarity condition (1). It turns out that for the diagrams in question  $\varphi_{jj+n} \neq 0$  only if the amplitude  $f_{jm}$  of the diagram of Fig. 4b is continued from the

region of small values of  $s_{13}$ . This fact is later manifest in the fact that of all the diagrams of Fig. 13 there is only one diagram, c (which contains the amplitude of Fig. 14b), having a Mandelstam branch point.

In Sec. 4 we investigate the unitarity condition for the amplitudes  $f_{jm}$  and  $\varphi_{jj+n}$  with respect to the energy of the pair of produced particles. For complex  $j$ , and for a function  $f_{jm}$  which increases slowly in  $j$  at small values of one of the pair energies, the unitarity condition with respect to this energy has a simple form. At low values of the pair energy, it coincides in form with the unitarity condition for physical  $j$ . At higher energies, the unitarity condition contains additions connected with the hooking of the singularities of the integrand by the integration contour. Of course, these additions vanish for physical values of  $j$ . Thus, to study the different pair interactions of the produced particles we shall make use of continuations of  $f_{jm}$  in  $j$ , which increase slowly for small values of the corresponding pair energies.

In Sec. 4 we consider also the unitarity condition in the pair energy for the amplitudes  $\varphi_{jj+n}$ . Its structure confirms the statement made in an earlier paper [3], that  $\varphi_{jj+n}$  has a pole in  $j$ , connected with the paired interaction of the produced particles. In the conclusion of the section we discuss those diagrams which lead to Mandelstam branch points.

In Sec. 5 we obtain the exact form of the three-particle contribution to the unitarity condition for complex  $j$  and for several simple Feynman diagrams (Fig. 16). The construction of these unitarity conditions is equivalent to the calculation of the Mandelstam spectral functions of the corresponding diagrams. Unlike the unitarity condition in the pair energy, we cannot propose a general prescription for writing down the three-particle unitarity condition. In particular, we do not know which particular continuations of  $f_{jm}$  arise for diagrams which are more complicated than Fig. 16. We see, however, that the quantities  $\varphi_{jj+n}$  introduced in (1) actually exist and have the necessary properties. This is all that is needed for the understanding of the mechanism of occurrence of Mandelstam branch points.

## 2. ANALYTIC CONTINUATION OF THE THREE-PARTICLE AMPLITUDES $f_{jm}$ IN $j$

For integral values of the total angular momentum  $j$  and its projection  $m$  on the momentum of one of the three produced particles, the three-particle partial amplitudes are determined by an

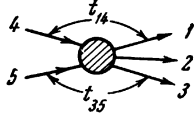


FIG. 1

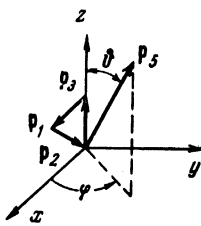


FIG. 2

integral of an invariant amplitude for the conversion of two particles into three (Fig. 1)

$$f_{jm}(s_{12}, s_{13}, s_{23}) = \int \frac{d\Omega}{4\pi} e^{-im\varphi} P_{jm}(z) A(t_{14}, t_{35}, s_{12}, s_{13}, s_{23}). \quad (2)$$

Here  $z = \cos \vartheta$ ,  $\vartheta$  and  $\varphi$  are the angles of the momentum  $p_5$  relative to the motion of the particles 4 and 5 in the initial state (Fig. 2). The invariant amplitude  $A$  depends on the two momentum transfers  $t_{14}$  and  $t_{35}$ , and on the pair energies  $s_{12}$ ,  $s_{13}$ , and  $s_{23}$  of the three produced particles.

In the earlier paper [3], the unitarity condition (1) was written with the aid of amplitudes  $f_{jm}$  obtained by continuation in  $j$  from integer  $j$  at fixed integer  $m$ . We shall now show how this continuation is actually realized. In continuing the two-particle partial amplitudes  $f_j(s)$  in  $j$ , we impose the condition that there be no singularities at large  $\operatorname{Re} j$ , and that there be a decrease in the right half-plane of  $j$  in any direction not parallel to the imaginary axis. We shall show later that no such continuation exists for the amplitudes  $f_{jm}$ , even in the case of the simplest diagrams. It is reasonable here to seek a continuation of  $f_{jm}$  which, to be sure, increases in the right half-plane, but does so in the minimum possible manner. We can hope that such amplitudes make it easiest to construct the three-particle contribution to the unitarity condition for  $f_j(s)$ , which should already decrease in the entire right half-plane of  $j$ . In addition, as will be shown later, the unitarity condition in the pair energy can be continued for such amplitudes to complex  $j$  in a simple fashion.

For an unambiguous choice of the continuation of  $f_{jm}$  to complex  $j$  with minimum growth, we can use the following theorem. There exists only one analytic function  $j$ , which assumes specified values at integer points, which has no singularities for sufficiently large  $\operatorname{Re} j$ , and which grows more slowly than  $\exp(\pi |\operatorname{Im} j|)$  in the right half plane (including directions parallel to the imaginary axis). If there were two such functions, then their differences, divided by  $\sin \pi j$ , would have no singularities for sufficiently large  $\operatorname{Re} j$ , and would decrease exponentially in the entire right half-

plane, including both directions parallel to the imaginary axis. According to the Carleman theorem (see, for example, [4]), such a function vanishes identically. In perfect analogy, for the continuation from even (or odd)  $j$  to be unique, the function should increase more slowly than  $\exp(\pi |\operatorname{Im} j|/2)$ . Inasmuch as the amplitudes  $f_{jm}$  are connected by the unitarity condition with the two-particle amplitudes  $f_j(s)$ , which call for introduction of a signature in  $j$ , we shall continue also the  $f_{jm}$  separately from even and odd  $j$ , stipulating that  $|f_{jm}| < \exp(\pi |\operatorname{Im} j|/2)$ .

To continue the integral (2) in  $j$  with integer  $m$ , we replace, in analogy with the continuation of the two-particle amplitude, the quantity  $P_{jm}(z)$  under the integral sign in (2) by

$$P_{jm}(z) = i\pi^{-1} e^{i\pi m/2} [Q_{jm}(z + ie)] \quad (-1 < z <$$

Substituting (3) in (2) we obtain

$$f_{jm} = \frac{ie^{i\pi m/2}}{\pi} \left\{ \int_{-1}^{+1} \frac{dz}{2} Q_{jm}(z + ie) \int_0^{2\pi} \frac{d\varphi}{2\pi} e^{-im\varphi} A(z, \varphi) \right. \\ \left. - \int_{-1}^{+1} \frac{dz}{2} Q_{jm}(z - ie) \int_0^{2\pi} \frac{d\varphi}{2\pi} e^{-im(\varphi+\pi)} A(z, \varphi) \right\}. \quad (4)$$

$A(z, \varphi)$  contains a dependence on  $(1 - z^2)^{1/2}$  and  $\varphi$  only in the form of the product  $(1 - z^2)^{1/2} \cos \varphi$ . (This can be seen from the explicit expression for the momentum transfers  $t_{14}$  and  $t_{35}$ .) The first integral in (4) can be regarded as the integral over the upper edge of the cut  $(1 - z^2)^{1/2}$ . Then the second integral reduces, by making a change in the integration variable  $\varphi \rightarrow \varphi + \pi$ , to an integral over the lower edge, where  $(1 - z^2)^{1/2} < 0$ . We thus get

$$f_{jm} = \frac{ie^{i\pi m/2}}{\pi} \int_C \frac{dz}{2} Q_{jm}(z) A_m(z), \\ A_m(z) = \int_0^{2\pi} \frac{d\varphi}{2\pi} e^{-im\varphi} A(z, \varphi), \quad (5)$$

where the contour  $C$  is shown in Fig. 3.

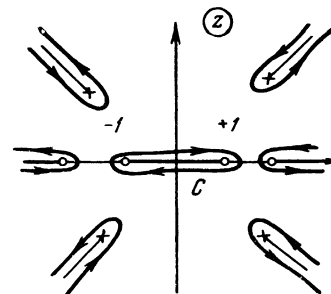


FIG. 3

The function  $A_m(z)$  has complex singularities in  $z$  (even for the simplest diagrams), both in the right and left half-planes. We obtain the continuation of  $f_{jm}$  to complex  $j$  by unfolding the contour of integration, for integer  $j$ , around the singularities of  $A_m(z)$ , after which  $j$  can already be regarded as arbitrary. (When  $j$  is sufficiently large, the integral along the large circle vanishes.) If the function  $A_m(z)$  has no singularities in the left half-plane of  $z$ , then the obtained continuation satisfies the uniqueness criterion formulated above ( $|f_{jm}| < \exp(\pi|\operatorname{Im} j|/2)$  as  $j \rightarrow \infty$  in the right half-plane.) If  $A_m(z)$  has singularities in  $z$  when  $\operatorname{Re} z < 0$ , then it is necessary to introduce a signature in  $j$ , projecting the contours along the corresponding cuts onto the right half plane with the aid of the substitution  $z \rightarrow -z$ .

To write down the unitarity condition (1) in [3], we needed not only the amplitudes  $f_{jm}$  with complex  $j$  and integer  $m$ , but also the functions  $\varphi_{jj+n}$ , obtained by continuing the functions  $f_{jj+n}$  in  $j$  from integer  $j$  of foreign signature. We shall not dwell here on the properties of this continuation in general form, and explain them when dealing with the concrete diagrams.

### 3. SIMPLEST DIAGRAMS

Let us consider the three-particle amplitudes corresponding to the diagrams shown in Fig. 4. For a single-pole diagram (Fig. 4a), the amplitude  $f_{jm}$  has a specially simple form, if  $m$  represents the projection of the total angular momentum on the momentum of the particle 3. It is easy to see that in this case (apart from a constant factor):

$$A_m(z) = \frac{1}{2p_3p_5} \delta_{m0} \frac{1}{z_{30} - z}. \quad (6)$$

Here  $z$  is the angle between the initial momentum  $p_5$  and the final momentum  $p_3$ , and

$$z_{30} = \frac{m^2 - m_3^2 - m_5^2 + 2p_{30}p_{50}}{2p_3p_5} > 1, \quad (7)$$

where  $m_3$ ,  $m_5$ , and  $m$  are the masses of the third, fifth, and intermediate particles, while  $p_{30}$  and  $p_{50}$  are the energies of the third and fifth particles. Substituting (6) in (5), we obtain

$$f_{jm} = \frac{1}{2p_3p_5} \delta_{m0} Q_j(z_{30}). \quad (8)$$

As seen from (8),  $f_{jm}$  decreases in this case in the right half plane of  $j$ .

Expression (8) for  $f_{jm}$  corresponds to the fact that the momentum  $p_3$  is chosen along the  $Z$  axis of the coordinate system. In investigating the uni-

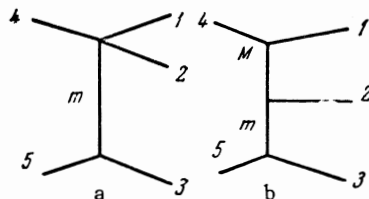


FIG. 4

tarity condition in the pair energies for  $f_{jm}$  we shall need in the future the amplitudes  $f_{jm}$  for which  $m$  is the projection of the momentum  $j$  on the different momenta  $p_1$ ,  $p_2$ , and  $p_3$ . Since the momenta  $p_1$  and  $p_2$  are equivalent for the diagram of Fig. 4a, we align the  $Z$  axis, with, say,  $p_2$ . The amplitudes  $f'_{jm}$  are then expressed in terms of  $f_{jm}$  for integer  $j$  in the following manner:

$$f'_{jm} = \sum_{m'=-j}^j P_{mm'}^j(z_{23}) f_{jm'} = P_{jm}(z_{23}) \frac{1}{2p_3p_5} Q_j(z_{30}), \quad (9)$$

where  $z_{23}$  is the cosine of the angle between the momenta  $p_2$  and  $p_3$ . The  $P_{mm'}^j(z_{23})$  coincide, apart from a normalization factor, with the well known functions  $d_{mm'}^j$  [5]:

$$P_{mm'}^j(z_{23}) = \left[ \frac{\Gamma(j+m+1)\Gamma(j-m'+1)}{\Gamma(j-m+1)\Gamma(j+m'+1)} \right]^{1/2} d_{mm'}^j(z_{23}). \quad (10)$$

Expression (9) can be continued directly to complex  $j$ , but it does not satisfy the requirement formulated above ( $|f'_{jm}| < \exp(\pi|\operatorname{Im} j|/2)$ ) in the entire physical region, but only when  $z_{23} > 0$ . We can continue (9) analytically in  $z_{23}$  into the region  $z_{23} < 0$ . We thus define uniquely the function  $f'_{jm}$  in the entire physical region, in some part of which ( $z_{23} < 0$ ) it will increase more rapidly when  $\exp(\pi|\operatorname{Im} j|/2)$ . We could have proceeded differently. For  $z_{23} < 0$ , continuing  $f'_{jm}$  separately from even and odd  $j$ , we can determine

$$f'_{jm} = \pm (-1)^m P_{jm}(-z_{23}) Q_j(z_{30}) / 2p_3p_5. \quad (9a)$$

The upper and lower signs correspond to positive and negative signatures. The function (9a) behaves in the required manner when  $z_{23} < 0$ , but increases more rapidly than  $\exp(\pi|\operatorname{Im} j|/2)$  when  $z_{23} > 0$ . Thus, even for the simplest diagram it is impossible to construct a single analytic function on the angular momentum  $j$  and of the pair energies in the entire physical region, satisfying the limitations imposed on the growth. This property has resulted here from the projection of the momentum on an inconvenient axis, but we shall show below, by considering more complicated diagrams, that it has a rather general character. It will therefore be necessary in the future to construct several dif-

ferent continuations of  $f_{jm}$ , analogous to (9) and (9a), each of which does not increase too rapidly only in a definite region of values of the pair energies.

We now proceed to consider the two-pole diagram in Fig. 4b. We first determine  $f_{jm}$  when the Z axis is taken to be in the direction of the momentum of the third particle. Simple calculations lead us to the following expression for  $A_m(z)$ :

$$\begin{aligned} A_m(z) &= \int_0^{2\pi} \frac{d\varphi}{2\pi} \frac{1}{4p_1 p_3 p_4 p_5}, \\ &\frac{1}{z_{30} - z} \frac{e^{-im\varphi}}{z_{10} + z_{13}z + [(1 - z_{13}^2)(1 - z^2)]^{1/2} \cos \varphi} \\ &= (-1)^m \frac{1}{4p_1 p_3 p_4 p_5} \frac{1}{z_{30} - z} \frac{1}{K^{1/2}(z, -z_{13}, z_{10})} \\ &\times \left[ \frac{z_{10} + z z_{13} + K^{1/2}(z, -z_{13}, z_{10})}{[(1 - z^2)(1 - z_{13}^2)]^{1/2}} \right]^{-im} \\ K(z, -z_{13}, z_{10}) &= z^2 + z_{13}^2 + z_{10}^2 + 2z z_{13} z_{10} - 1. \end{aligned} \quad (11)$$

Here  $z_{13}$  is the cosine of the angle between  $\mathbf{p}_1$  and  $\mathbf{p}_3$ , while  $z_{10}$  and  $z_{30}$  are defined in analogy with (7).

Following the prescription of the preceding section, we should unfold the integration contour C around the singularities of  $A_m(z)$ . It follows from (11) that  $A_m(z)$  has, besides a cut between  $-1$  and  $+1$  inside the contour C, a pole at  $z = z_{30}$  and two complex-conjugate branch points at

$$z = -z_{10} z_{13} \pm i[(1 - z_{13}^2)(z_{10}^2 - 1)]^{1/2} \quad (12)$$

(see Fig. 5). By choosing the cuts as shown in Fig. 5 we get  $K^{1/2}(z, -z_{13}, z_{10}) > 0$  for real  $z$ .

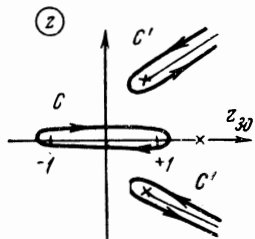


FIG. 5

The contribution to  $f_{jm}$  from the residue at the pole decreases for large  $j$  like  $\exp(-j\alpha_{30})$ , where  $\cosh \alpha_{30} = z_{30}$ . When  $j \rightarrow \infty$ , the integrals along the cuts from the branch points (12) behave like  $\exp[-j(\alpha_{10} \pm i\beta_{13})]$ , where  $\cosh \alpha_{10} = z_{10}$  and  $\cos \beta_{13} = -z_{13}$ . When  $z_{13} < 0$  we obtain the required continuation, which increases more slowly than  $\exp(\pi |\operatorname{Im} j|/2)$ . This is one of the possible continuations. Another continuation is obtained if

we start from the region  $z_{13} > 0$ . In this case the branch points are in the left half plane of  $z$ , so that for the continuation in  $j$  it becomes necessary, even for integer  $j$ , to separate the factor  $(-1)^j$  from the integrals along the cuts and replace it by  $\pm 1$ , depending on the parity of  $j$  (i.e., introduce a signature with respect to  $j$ ).

Assume now that the direction of the Z axis is that of the momentum of the second particle. Unlike the case of the single-pole diagram, it is simpler here not to use the recalculation formula (9), and to calculate  $f_{jm}$  anew, starting directly from the diagram of Fig. 4b. We obtain for  $A_m(z)$  in this case

$$\begin{aligned} A_m(z) &= \frac{1}{4p_1 p_3 p_4 p_5} \frac{(1 - z^2)^{m/2}}{(z_{10} + z_{12}z)(1 - z_{23}^2)^{1/2} - (z_{30} - z_{23}z)(1 - z_{12}^2)^{1/2}} \\ &\times \left\{ \frac{(1 - z_{23}^2)^{1/2}}{K^{1/2}(z, z_{23}, z_{30})} \left[ \frac{z_{30} - z_{23}z + K^{1/2}(z, z_{23}, z_{30})}{(1 - z_{23}^2)^{1/2}} \right]^{-m} \right. \\ &\left. - \frac{(1 - z_{12}^2)^{1/2}}{K^{1/2}(z, -z_{12}, z_{10})} \left[ \frac{z_{10} + z_{12}z + K^{1/2}(z, -z_{12}, z_{10})}{(1 - z_{12}^2)^{1/2}} \right]^{-m} \right\}. \end{aligned} \quad (13)$$

$A_m(z)$  has now only the branch points connected with the cuts of the two  $K^{1/2}$

$$z = z_{23} z_{30} \pm i[(1 - z_{23}^2)(z_{30}^2 - 1)]^{1/2}, \quad (14a)$$

$$z = -z_{12} z_{10} \pm i[(1 - z_{12}^2)(z_{10}^2 - 1)]^{1/2}. \quad (14b)$$

The function  $A_m(z)$  (13) has no pole due to the vanishing of the denominator preceding the curly brackets, since the residue is equal to zero. The singularities (14a) and (14b) can again be situated either in the right or in the left half-planes of  $z$ , depending on the signs of  $z_{12}$  and  $z_{23}$ .

The regions of positive and negative values of  $g_{ik}$  are best illustrated with the aid of a Dalitz diagram (Fig. 6). In Fig. 6 the squares of the relative energies of the particles  $s_{12}$ ,  $s_{13}$ , and  $s_{23}$  are measured from the continuous straight lines in the directions indicated by the arrows. The straight lines themselves correspond to the threshold values of the pair energies, while the relative momenta are  $q_{12} = 0$ ,  $q_{13} = 0$ , and  $q_{23} = 0$ .

The dashed lines correspond to the maximum values of the pair energies  $s_{12}$ ,  $s_{13}$ , and  $s_{23}$ , when the respective momenta  $p_3$ ,  $p_2$ , and  $p_1$  vanish. The physical region in which  $|z_{ik}| < 1$  is located inside the circle<sup>1)</sup>. Using Appendix 1, we can easily

<sup>1)</sup>In fact, the physical region is bounded by a complicated curve, which is inscribed in both triangles shown in the figure. For brevity we call it a circle.

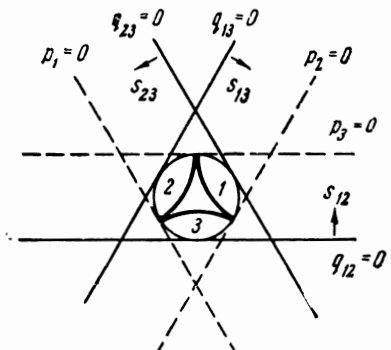


FIG. 6

verify directly that  $z_{12} > 0$  only in the region marked No. 3 in the figure, corresponding to small values of  $s_{12}$ ;  $z_{12} > 0$  in region 2, and  $z_{23} > 0$  in region 1. In the central region all  $z_{ik} < 0$ .

We see from (14a) and (14b) that the branch points  $A_m(z)$  are in the right half-plane when  $z_{23} < 0$  and  $z_{12} < 0$ , i.e., in region 1. In all the other regions, at least one of the pair of the singularities (14a) and (14b) is located in the left half-plane of  $z$ . As already explained above, each of these cases has its own continuation in  $j$ , which then extends to the entire physical region. We shall be interested in what follows in the three continuations defined initially in regions 1, 2, and 3. The continuation which is constructed from the central region will not do for us. We note that when  $f_{jm}$  is continued from region 1, we need not introduce any signature at all. Upon continuation from region 3, when both singularities in  $z$  lie in the left half-plane, it is necessary to introduce a signature. In this case, however, the entire role of the signature reduces to the fact that the continuation from odd  $j$  differs only in sign from continuation from even  $j$ . Such a situation, of course, will always take place when all the singularities of  $A_m(z)$  lie in the left half-plane. We note that here, as in the absence of a signature, the continuation from all  $j$  calls for introducing only one independent analytic function of  $j$ . Finally, let us consider the continuation from region 2. In this case the singularities (14a) and (14b) lie in different half-planes and the determination of  $f_{jm}$  for complex  $j$  calls for the introduction of a signature, and continuation from even and odd  $j$  leads to two entirely different analytic functions.

We have thus constructed the quantities  $f_{jm}$  for the diagrams of Fig. 4a and b for all complex  $j$  and integer positive  $m$ . It is easy to note that  $f_{jm} = 0$  for physical integer  $j < m$ , i.e., for  $j$  of their own signature. On the other hand, if we consider  $f_{jm}$  for integer  $j < m$  but foreign signature (for exam-

ple, we consider odd  $j$  when the continuation is carried out from even  $j$ ), then the  $f_{jm}$  may differ from zero. From expressions (9) and (9a) for the amplitudes  $f_{jm}$  of the single-pole diagram (Fig. 4a) we see that  $f_{jm} = 0$  for all positive integer  $j < m$ , independently of whether a signature is absent [formula (9)] or present [formula (9a)]. The same holds true also in the case of a two-pole diagram for continuations that go from regions 1 and 3. For these continuations, as for the single-pole diagram the signature is either entirely unnecessary, or reduces to a change in the over-all sign. The situation is different in the continuation of  $f_{jm}$  for a two-pole diagram from region 2. Here, by continuing  $f_{jm}$ , say, from even  $j$  we obtain for odd  $j < m$  values which differ from zero. These values are the basis for the construction of the functions  $\varphi_{jj+n}$ , obtained by continuation in  $j$  for a fixed difference  $m-j$ <sup>[3]</sup>. Let us calculate  $\varphi_{jj+n}$  explicitly for the case when the angular momentum is projected on the momentum of the particle 2. (The function  $\varphi_{jj+n}$  obtained when the angular momentum is projected on the momentum of the particles 1 and 3 will not be needed in what follows.)

The amplitudes  $f_{jm}$  for complex  $j$  and integer  $m$  are specified by four integrals of the function  $A_m(z)$  in (13), along cuts that travel from singularities (14a) and (14b). The expression for  $f_{jm}$  can in this case be written in the form

$$\begin{aligned} f_{jm} = & \int_{(14a)} Q_{jm}(z) (z^2 - 1)^{m/2} F_1(z) dz \\ & - \int_{(14b)} Q_{jm}(z) (z^2 - 1)^{m/2} F_2(z) dz, \end{aligned} \quad (15)$$

where  $F_1(z)$  and  $F_2(z)$  correspond to two terms in formula (13). The integrals are taken over the cuts connected respectively with singularities (14a) and (14b). Singularities (14a) lie in the left half-plane. (We recall that we start the continuation in region 2, where  $z_{12} < 0$ ,  $z_{23} < 0$ , and  $z_{13} > 0$ .) Therefore, to obtain a slowly growing continuation of  $f_{jm}$  ( $< \exp(\pi | \operatorname{Im} j | / 2)$ ) we can rewrite (15) for integer  $j$  (for concreteness, even) in the form

$$\begin{aligned} f_{jm} = & - \int_{(14a)} Q_{jm}(-z) (z^2 - 1)^{m/2} F_1(z) dz \\ & - \int_{(14b)} Q_{jm}(z) (z^2 - 1)^{m/2} F_2(z) dz. \end{aligned} \quad (16)$$

We now consider this expression for integer  $j < m$ . The function  $(z^2 - 1)^{m/2} Q_{jm}$  is in this case a polynomial in  $z$  of degree  $m-j-1$ . Therefore the contours in formula (16) can be transferred to the pole of the function  $F_1(z)$  and  $F_2(z)$ . The position of this pole, as can be seen from (13) is

$$\begin{aligned} z_0 &= \frac{z_{30}(1 - z_{12}^2)^{1/2} - z_{10}(1 - z_{23}^2)^{1/2}}{z_{12}(1 - z_{23}^2)^{1/2} + z_{23}(1 - z_{12}^2)^{1/2}} \\ &= \frac{z_{10}(1 - z_{23}^2)^{1/2} - z_{30}(1 - z_{12}^2)^{1/2}}{(1 - z_{13}^2)^{1/2}}. \end{aligned} \quad (17)$$

Then

$$f_{jm} = 2\pi i Q_{jm}(z_0) (z_0^2 - 1)^{m/2} [f_1(z_0) (-1)^{j+1} + f_2(z_0)], \quad (18)$$

where  $f_1(z_0)$  and  $f_2(z_0)$  are the residues of  $F_1(z)$  and  $F_2(z)$  at  $z = z_0$ .

From the explicit expression for the functions  $F_1$  and  $F_2$  we readily see that  $f_1(z_0) = f_2(z_0)$ . Here, as expected,  $f_{jm} = 0$  for even  $j$  that are smaller than  $m$ . Using the value of  $f_{jm}$  for odd  $j < m$  and putting  $m - j = n$ ,  $n = 1, 2, \dots$ , we can now construct the quantity  $\varphi_{jj+n}$  by continuation in  $j$ :

$$\begin{aligned} \varphi_{jj+n} &= 4\pi i (z_0^2 - 1)^{(j+n)/2} Q_{jj+n}(z_0) f_1(z_0) \\ &= \frac{1}{4p_1 p_3 p_4 p_5} 2(z_0^2 - 1)^{(j+n)/2} \frac{Q_{jj+n}(z_0)}{K^{1/2}(z_{30}, -z_{13}, z_{10})} \\ &\times \left[ \frac{K^{1/2}(z_{30}, -z_{13}, z_{10}) - z_{10} z_{23} - z_{30} z_{12}}{(1 - z_{13}^2)^{1/2}} \right]^{-j-n}. \end{aligned} \quad (19)$$

Expression (19) satisfies the requirement that it make a decreasing contribution to the integrand of the unitarity condition (1), at least for small  $s_{13}$ , where the sum over  $n$  is meaningful. In order to verify this, we note that the function  $(z_0^2 - 1)^{j+n/2} Q_{jj+n}(z_0)$  is a polynomial even for complex  $j$ :

$$\begin{aligned} (z_0^2 - 1)^{(j+n)/2} Q_{jj+n}(z_0) &= e^{i\pi(j+n)} 2^{j+n-1} \Gamma(j+n+1, -2j-n, \\ &-j-n+1, 1/2 - z_0/2), \end{aligned} \quad (20)$$

where  $F$  is the hypergeometric function. The polynomial (20) coincides, apart from a factor, with the Gegenbauer polynomial  $C_{n-1}^{-j-n+1/2}(z_0)$ . For large  $j$ , the quantity  $\varphi_{jj+n}$  in region 2 (Fig. 6), from which we start the continuation, contains an exponentially decreasing factor  $a^{-j}$ , where  $a$  is the expression in the square brackets (it is easy to show that in this region  $a > 1$ ). It is not difficult to check, further, that the remaining factors that depend on  $j$  result only in a power-law dependence on  $n$  in the unitarity condition (1) ( $\sim j^{n-3/2}$ ).

Let us summarize briefly the results of the present section. We have shown that there exist several possible continuations of the partial amplitudes  $f_{jm}$  to complex  $j$ . Each of these continuations satisfies the limitations imposed at the be-

ginning of the paper, that the growth as  $j \rightarrow \infty$  be only a definite region of values of the pair energies. The constructed quantities can then be extended, by analytic continuation in the energies, to cover the entire physical region. We have also found the functions  $\varphi_{jj+n}$ , which determine the addition to the unitarity condition (1) for the diagram of Fig. 4b. These functions turn out to differ from zero only for continuation from the region corresponding to small values of the pair energy of particles 1 and 3. The  $\varphi_{jj+n}$  always vanish for the diagram of Fig. 4a.

#### 4. UNITARITY CONDITION IN THE PAIR ENERGIES FOR THREE-PARTICLE AMPLITUDES

We have previously employed<sup>[3]</sup> the unitarity condition for the three-particle amplitudes  $f_{jm}$  in terms of the pair energy of the two produced particles. Since we did not determine in detail in<sup>[3]</sup> the analytic continuation of the amplitudes  $f_{jm}$  in  $j$ , the expression written out there for the unitarity condition was quite arbitrary. We now investigate the structure of the unitarity condition with respect to the pair energy more thoroughly, using the results of the preceding section. We consider the diagram shown in Fig. 7. The unitarity condition corresponding to this diagram, for physical  $j$  and  $m$ , is of the form<sup>[3]</sup>:

$$\begin{aligned} \frac{1}{2i} [f_{jm}(s_{12} + ie, x) - f_{jm}(s_{12} - ie, x)] \\ = \frac{q_{12}}{8\pi \sqrt{s_{12}}} \int_{-1}^{+1} dx' f_m(s_{12} - ie, x, x') f_{jm}(s_{12} + ie, x'). \end{aligned} \quad (21)$$

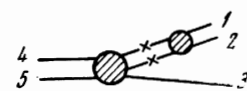


FIG. 7

Here  $m$  is the projection of the angular momentum of particle 3<sup>2)</sup>,  $\sqrt{s_{12}}$  is the total energy of the particles 1 and 2 in their c.m.s.,  $x$  is the cosine of the angle between the relative momentum  $q_{12}$  of the particles 1 and 2 in the final state and the momentum  $p_3$  of the third particle, and  $x'$  is the same for the particles in the intermediate state. We note that, for a specified total energy, any variable describing the kinematics of the three particles can,

<sup>2)</sup>Here and throughout we diagonalize the unitarity condition with respect to  $m$ , projecting the total angular momentum on the momentum of the non-interacting particle.

of course, be expressed in terms of  $s_{12}$  and  $x$  (see Appendix 1). The function  $j_m$  in the integrand of (21) is of the form

$$f_m(s_{12}, x, x') = \int_0^{2\pi} \frac{d\varphi}{2\pi} e^{-im\varphi} a(s_{12}, z), \quad (22)$$

where  $a(s_{12}, z)$  is the amplitude for the scattering of particles 1 and 2, while the cosine  $z$  of the scattering angle is expressed in terms of  $x, x'$ , and  $\varphi$  by:

$$z = xx' + [(1-x^2)(1-x'^2)]^{1/2} \cos \varphi. \quad (23)$$

We have shown in the preceding section that the amplitude  $f_{jm}$  can be continued to complex  $j$  by several methods, starting from different regions in the pair energies. We consider first the region of small  $s_{12}$ , more precisely region 3 in Fig. 6. All the points of the contour of integration with respect to  $x'$  lie in this case also in region 3. (The integration with respect to  $x'$  is equivalent, of course, to integration along the straight line  $s_{12} = \text{const}$  between the limits of the circle.) If we consider a continuation of  $f_{jm}$  which grows weakly in region 3, then the unitarity condition in this region can be continued to complex  $j$  directly in the form (21). It is then sufficient to regard all the amplitudes  $f_{jm}$  in (21) as continued to complex  $j$ . Since both the left and the right sides of the equation increase here more slowly than  $\exp(\pi |\text{Im } j|/2)$ , the continuation (21) in  $j$  will be unique. The form of the unitarity conditions for the continuations of  $f_{jm}$  which increase slowly in other regions cannot be obtained in region 3 directly, since these continuations increase more rapidly than  $\exp(\pi |\text{Im } j|/2)$  in region 3.

The extension of the unitarity condition (21) to the entire physical region can now be obtained by analytic continuation in  $s_{12}$  from the region of small  $s_{12}$ . If we are interested in the unitarity conditions with respect to other pair energies, for example  $s_{13}$ , then we must begin the continuation from the region of small values of  $s_{13}$ , i.e., from region 2.

To ascertain the form of the unitarity condition (21) for large values of  $s_{12}$ , we turn to the concrete diagrams shown in Fig. 8. For this case, (21) takes the form

$$\frac{1}{2i} [f_{jm}(s_{12} + ie, x) - f_{jm}(s_{12} - ie, x)]$$

$$= \frac{q_{12}}{8\pi \sqrt{s_{12}}} \int_{-1}^{+1} \frac{dx'}{2} f_m(s_{12} - ie, x, x') f_{jm}^{(0)}(s_{12} + ie, x'), \quad (24)$$

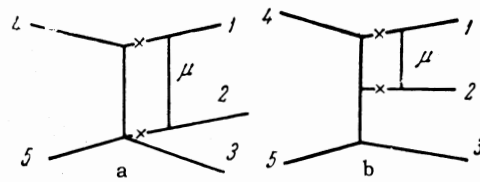


FIG. 8

where the function  $f_m$  is equal to

$$f_m = \frac{1}{2q_{12}^2} \frac{1}{K^{1/2}(\xi, x, x')} \left[ \frac{\xi - xx' + K^{1/2}(\xi, x, x')}{[(1-x^2)(1-x'^2)]^{1/2}} \right]^{-m},$$

$$\xi = 1 + \frac{\mu^2}{2q_{12}^2}. \quad (25)$$

Here  $\mu$  is the mass of the particle shown in Fig. 8

The continuation of (24) to the region of  $s_{12}$  turns out to be perfectly analogous for diagrams 8a and b, so that we shall consider below only the more complicated case of the diagram in Fig. 8b. The quantity  $f_{jm}^{(0)}$  is here the partial amplitude of the two-pole diagram of Fig. 4b, which was investigated in the preceding section [see formula (11)]:

$$f_{jm}^{(0)} = \frac{(-1)^m}{4p_1 p_3 p_4 p_5} \left\{ Q_{jm}(z_{30}) (z_{30}^2 - 1)^{m/2} \frac{1}{K^{1/2}(z_{30}, -z_{13}, z_{10})} \right. \\ \times \left( \frac{z_{30} z_{13} + z_{10} + K^{1/2}(z_{30}, -z_{13}, z_{10})}{(1 - z_{13}^2)^{1/2}} \right)^{-m} \\ - \frac{1}{2\pi i} \int dz Q_{jm}(z) (z^2 - 1)^{m/2} \frac{1}{K^{1/2}(z, -z_{13}, z_{10})} \\ \times \left( \frac{z z_{13} + z_{10} + K^{1/2}(z, z_{10}, -z_{13})}{(1 - z_{13}^2)^{1/2}} \right)^{-m} \frac{1}{z_{30} - z}. \quad (26)$$

The contour  $C'$  is shown in Fig. 5.

As shown above, for small  $s_{12}$  the integration with respect to  $x'$  in the integral of (24) is carried out from  $-1$  to  $+1$ , and all the singularities of the integrand are located outside the integration contour. The question is whether the singularities of the integrand with respect to  $x'$  can approach the contour of integration with respect to  $x'$  when  $s_{12}$  increases and link with this contour. Since this is actually possible (this will be shown later), the second question is tantamount to asking whether singularities in  $s_{12}$  appear in this case, i.e., whether a unique continuation of the unitarity condition (24) to all physical values of  $s_{12}$  is possible. We shall show that there are no singularities in  $s_{12}$  and that the continuation is possible.

Let us consider the singularities of the integrand in expression (24) with respect to  $x'$ . For physical values of  $s_{12}$  and  $x$ , the function  $f_m(s_{12}, x, x')$  has a complex singularity, corresponding to the vanishing of  $K(x, x', \xi)$ , which does not fall on the inte-

gration contour. Let us consider the function  $f_{jm}^0(s_{12}, x')$  defined by formula (26). The quantities  $z_{10}$ ,  $z_{30}$ ,  $z_{13}$ ,  $p_1$ , and  $p_3$  are expressed in terms of  $s_{13}$  and  $x'$  in accordance with the formulas of Appendix 1 (where  $x$  must of course be replaced by  $x'$ ). When  $x' = x_1^+$  and  $x' = x_1^-$ , the momentum is  $p_1 = 0$  and the cosines  $z_{10}$  and  $z_{13}$  become infinite. For  $z_{13}$  this is valid along the entire line  $p_1 = 0$ , except the point where this line is tangent to the circle (Fig. 9), where the value of  $z_{13}$  is indeterminate. The points  $x' = x_1^+$  and  $x' = x_1^-$  are singular for the functions  $f_{jm}^{(0)}$  and for the entire integrand of (24). From formula (A.4) of Appendix 1 we see that for small  $s_{12}$  both singularities  $x_1^+$  and  $x_1^-$  are to the right of the contour of integration with respect to  $x'$ . For certain values  $s_{12} = s_{12}^{(1)}$  the line  $p_1 = 0$  is tangent to the circle, and this corresponds to the fact that the singularity  $x_1^-$  approaches  $x' = 1$ . With further increase of  $s_{12}$ , it links with the contour of integration in (24) and again goes off to the right. Depending on the manner of circuiting around the  $s_{12} = s_{12}^{(1)}$ , the singularity  $x_1^-$  can go around  $+1$  from below (as shown in Fig. 10) or from above. As a result, when  $s_{12} > s_{12}^{(1)}$  there appears in the unitarity condition (24) an added term equal to the integral over the first part of the contour. In Fig. 9 this corresponds to the fact that integration with respect to  $x'$  is now carried out not only over the physical region (between the boundaries of the circle), but also between the boundary of the circle and the line  $p_1 = 0$ .

To check that  $s_{12} = s_{12}^{(1)}$  is not a singular point, it is necessary to verify that the integral over the

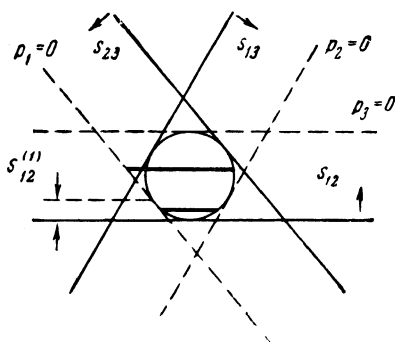


FIG. 9

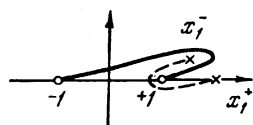


FIG. 10

hooked part of the contour does not depend on the method of going around this point. A direct calculation, given in Appendix 2, shows that this is indeed the case. For the addition to the unitarity condition (24) we obtain the expression

$$\begin{aligned} \Delta &= \frac{q_{12}}{8\pi\sqrt{s_{12}}} \int_{+1}^{x_1^-} \frac{dx'}{2} f_m(s_{12}, x, x') [f_{jm}^{(0)+} - f_{jm}^{(0)-}] \\ &= \theta(s_{12} - s_{12}^{(1)}) \sin \pi j \frac{q_{12}}{8\pi\sqrt{s_{12}}} \int_{-1}^{x_1^-} \frac{dx'}{2} \left\{ \frac{1}{2q_{12}^2 K^{1/2}(\zeta, x, x')} \right. \\ &\quad \times \left[ \frac{\zeta - xx' + K^{1/2}(\zeta, x, x')}{[(1-x^2)(-1+x'^2)]^{1/2}} \right]^{-m} \left\{ \frac{(-1)^m}{4p_1 p_3 p_4 p_5 \pi} \right. \\ &\quad \times \left. \int_L dz Q_{jm}(z) (z^2 - 1)^{m/2} \frac{1}{(z_{10} + z) K^{1/2}(z, z_{10}, z_{13})} \right. \\ &\quad \times \left. \left( \frac{-zz_{13} + z_{10} + K^{1/2}(z, z_{10}, z_{13})}{(z_{13}^2 - 1)^{1/2}} \right)^{-m} \right\}. \end{aligned} \quad (27)$$

Here  $f_{jm}^{(0)+}$  and  $f_{jm}^{(0)-}$  are the values of  $f_{jm}^{(0)}$  on opposite sides of the cut from the point  $x_1^-$  (Fig. 10), the contour  $L$  encloses the cut  $K^{1/2}(z, z_{10}, z_{13})$  drawn from  $z = z_{10}z_{13} + [(z_{10}^2 - 1)(z_{13}^2 - 1)]^{1/2}$  to  $+\infty$ ;  $K^{1/2}(z, z_{10}, z_{13}) > 0$  on the upper edge; the integration is carried out in a direction such that the start of this cut is circled clockwise. As expected,  $\Delta$  vanishes for integer  $j$ , for in this case the point  $x_1^-(p_1 = 0)$  is not a singularity.

We note that for non-integer  $j$  the function  $f_{jm}^{(0)}$  has as  $p_1 \rightarrow 0$  a singularity like  $(p_1)^{2j+3}$ . Therefore, at first glance the point  $x' = x_1^-$  is a root-type branch point even for integer  $j$ . However, for integer  $j$  the coefficient of  $p_1^{2j+3}$  vanishes, and the point  $x_1^-$  turns out to be in this case non-singular, as can be seen from expression (27) for the jump on the singularity.

We have discussed in detail the role of the singularity of  $f_{jm}^{(0)}$  when  $p_1 = 0$ . Another singularity of the function  $f_{jm}^{(0)}$  is the line  $p_3 = 0$ . This line, however, is reached in the continuation in  $s_{12}$  only for the maximum value of  $s_{12}$ , and is of no interest to us.

Concluding the discussion of the diagram of Fig. 8b, we note also that this diagram has for non-integer  $j$  additional singularities whose positions depend simultaneously on  $s_{12}$  and  $x$ . The occurrence of these singularities is explained in Appendix 3. Their trajectories touch the boundaries of the physical region, in the same manner as the lines  $p_i = 0$ . Therefore when writing down the unitarity conditions for more complicated diagrams, where the diagram of Fig. 8b itself is already integrated in phase volume, there should arise new

additions of the type (27), connected with the new singularities.

We now proceed to the unitarity condition for the diagram shown in Fig. 11, when particles 1 and 3 interact. The unitarity condition can be readily generalized here to include complex  $j$  for small values of  $s_{13}$  (region 2 in Fig. 6):

$$\begin{aligned} & \frac{1}{2i} [f_{jm}(s_{13} + i\epsilon, x) - f_{jm}(s_{13} - i\epsilon, x)] \\ &= \frac{q_{13}}{8\pi \sqrt{s_{13}}} \int_{-1}^{+1} \frac{dx'}{2} f_m(s_{13} - i\epsilon, x, x') f_{jm}^{(0)}(s_{13} + i\epsilon, x'). \end{aligned} \quad (28)$$

$x$  now denotes the cosine of the angle between  $\mathbf{q}_{13}$  and  $\mathbf{p}_2$ , and  $m$  is the projection of the angular momentum on the direction of  $\mathbf{p}_2$ . The function  $f_m$  is given by expression (25) with the substitution  $\mathbf{q}_{12} \rightarrow \mathbf{q}_{13}$ .

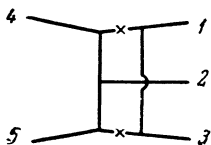


FIG. 11

As explained in the preceding section, in region 2 it becomes necessary to introduce a signature for the continuation of  $f_{jm}^{(0)}$ . The explicit form of  $f_{jm}^{(0)}$  is given in Appendix 4. When the continuation is made in  $s_{13}$ , when  $s_{13} = s_{13}^{(1)}$  and  $s_{13}^{(3)}$  (Fig. 12), the contour of integration with respect to  $x'$  is now linked at the points  $x' = 1$  and  $x' = -1$  by the singularities connected with the lines  $p_1 = 0$  and  $p_3 = 0$ . The expressions for the additions arising in unitarity condition (28) are also written out in Appendix 4. Their structure is similar to the added term (27) of the unitarity condition for the diagrams of Fig. 8b.

All the changes in the structure of the unitarity condition, considered so far, have been determined

by the overtaking of the contour of integration in (24) and (28) by singularities whose existence was not connected with the introduction of the signature. In the case of the diagram of Fig. 11, the need for introducing the signature leads to an additional singularity of the integrand of (28). This singularity arises when the pole  $z = z_0$  in expression (A.10) for  $f_{jm}^{(0)}$  (Appendix 4) collides with the singularities (14a) and (14b). Its trajectory, shown schematically in Fig. 12 by curve K, touches the physical region at the point A (at this point  $z_{10} = z_{30}$ , see Appendix 4) when  $s_{13} = s_{13}^{(0)}$ . For  $s_{13}^{(0)} > s_{13}^{(0)}$  the unitarity condition (28) for complex  $j$  acquires a new addition, which is described by expression (A.16) or Appendix 4. Unlike in the preceding additions, this addition no longer vanishes for all integer  $j$ , but only for integer  $j$  of its own signature (physical). The values of the pair energy  $s_{13}$ , at which the changes of the unitarity condition (28) take place ( $s_{13}^{(1)}, s_{13}^{(3)}, s_{13}^{(0)}$ ) are not singularities of the amplitude  $f_{jm}(s_{13}, x)$ . This follows directly from the formulas of Appendix 4.

We now proceed to the unitarity condition in the pair energies for the quantities  $\varphi_{jj+n}$ . It is easy to see that all the general arguments with respect to the pair unitarity condition for  $f_{jm}$ , given in the beginning of this section, are valid also for  $\varphi_{jj+n}$ . In writing down the unitarity condition for the diagram of Fig. 8 we started from the region of small values of  $s_{13}$  (region 3). For small values of  $s_{12}$ , the arrangement of the singularities is such that there is no need for introducing a signature, and therefore, as explained above,  $\varphi_{jj+n} = 0$ . For the diagram of Fig. 11, the continuation starts from region 2, where  $s_{13}$  is small. In this case the quantities  $f_{jj+n}$  differ from zero both for the simplest two-pole diagram and for the diagram of Fig. 11. The unitarity condition then takes the form<sup>[3]</sup>:

$$\begin{aligned} & \frac{1}{2i} [\varphi_{jj+n}(s_{13} + i\epsilon, x) - \varphi_{jj+n}(s_{13} - i\epsilon, x)] \\ &= \frac{q_{13}}{8\pi \sqrt{s_{13}}} \int_{-1}^{+1} \frac{dx'}{2} f_{j+n}(s_{13} - i\epsilon, x, x') \varphi_{jj+n}^{(0)}(s_{13} + i\epsilon, x'), \end{aligned} \quad (29)$$

where the functions  $\varphi_{jj+n}$  pertain to the diagram of Fig. 11, while  $\varphi_{jj+n}^{(0)}$  pertain to the simple two-pole diagram of Fig. 4b. The quantity  $f_{j+n}$  is determined by formula (23) with the substitution  $\mathbf{q}_{12} \rightarrow \mathbf{q}_{13}$  for  $m = j + n$ . From the explicit form of (19) for  $\varphi_{jj+n}^{(0)}$  it follows that the point  $p_1 = 0$  and  $p_3 = 0$  are now not singular, and therefore they do not link with the contour of integration with

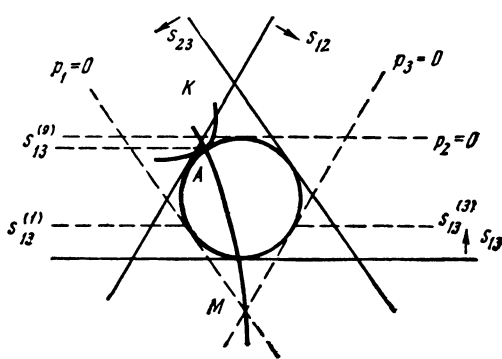


FIG. 12

respect to  $x'$ , as was the case for the quantities  $f_{jm}$ . However, the point  $x' = x_K(s_{13})$ , defined in Appendix 4, is as before a singularity of the integrand, and when  $s_{13} > s_{13}^{(0)}$  it hooks the contour of integration with respect to  $x'$  in (29). When  $s_{13} > s_{13}^{(0)}$ , the quantities  $\varphi_{jj+n}^{(0)}(s_{13}, x')$  become infinite on the boundary of the physical region ( $x' = +1$ ), since they contain the factor

$$\left( \frac{(1 - z_{13}^2)^{1/2}}{K^{1/2}(z_{30}, z_{10}, -z_{13}) - z_{10}z_{23} - z_{30}z_{12}} \right)^{j+n} \sim \left( \frac{1}{1 - x'^2} \right)^{(j+n)/2}$$

However, the integrand in (29) remains finite, since this growing factor is compensated by the zero of the function  $f_{j+n}$ , which is proportional near the boundary to  $(1 - x'^2)^{(j+n)/2}$ . Unlike the unitarity conditions for  $f_{jm}$ , the contour of integration in the unitarity conditions for  $\varphi_{jj+n}$  is overtaken for arbitrary  $j$ . This is connected with the fact that the quantities  $\varphi_{jj+n}$  are defined only with a signature, and a transition to the nonphysical  $j$  in the quantities  $f_{jm}$ . Therefore there are no physical values of  $j$  for them.

As  $s_{13}$  increases to the maximum value (the line  $p_2 = 0$ ), the singularity, which overtakes the contour of integration with respect to  $x'$  in (29), goes off to infinity. Along its way it can again, as explained in an investigation of the diagram of Fig. 8a, encounter the singularity of the function  $f_{j+n}$ , and this will lead to the appearance of singularities in  $\varphi_{j+n}$  for the diagram of Fig. 11. Such singularities, whose positions depend on  $s_{13}$  and  $x$ , will touch the boundary of the physical region ( $x = 1$ ) and cover the contours of integration in the three-particle unitarity condition (1) in the terms containing  $\varphi_{jj+n}$ .

Let us summarize the principal results obtained in the present section. We have shown that for continuations of  $f_{jm}$  and  $\varphi_{jj+n}$  to complex  $j$ , which increase slowly in  $j$  in the region of small values of one of the pair energies, there exists a simple unitarity condition with respect to this pair energy. We investigated then the continuations of these unitarity conditions in the pair energies to the entire physical region. It turns out that such continuations are unique (in view of the absence of additional singularities with respect to the energy for unphysical values of  $j$ ). However, the explicit form of the unitarity conditions is different in different regions in the pair energy, and includes integrations over unphysical values of the angles. In all the cases investigated by us, the modified region of integration turns out to be located inside a triangle and made up by the lines  $p_i = 0$  on the Dalitz diagram.

In [3] we wrote out a unitarity condition of type (29) without an analysis of the character of the continuation of the quantities  $\varphi_{jj+n}$ . It was shown in that paper that the quantity  $\varphi_{jj+n}$  has a pole in  $j$  when  $j = \alpha(s_{13}) - n$ , if the pair scattering amplitude of particles 1 and 3 has a Regge pole with trajectory  $\alpha(s_{13})$ . This is precisely the pole which generates the Mandelstam branch points when the functions  $\varphi_{jj+n}$  and  $\varphi_{j+n}^*$  are integrated with respect to  $d\Gamma_3$  in the three-particle unitarity condition (1). The fact that the unitarity condition has the usual form (the one used in [3]) for the amplitudes  $\varphi_{jj+n}$  when  $s_{13}$  is small proves the correctness of the deductions of [3] relative to the poles of  $\varphi_{jj+n}$ .

We now discuss briefly the Feynman diagrams which lead to the appearance of branch points. From the method of constructing the quantities  $\varphi_{jj+n}$  it is clear that for the existence of Mandelstam branch points it is necessary that the continuation of the amplitudes  $f_{jm}$  require the introduction of a signature in  $j$ . (We recall that in the opposite case the functions  $\varphi_{jm}$  with odd  $j < m$ , which serve as the basis for construction of the amplitudes  $\varphi_{jj+n}$ , are equal to zero.) We consider the diagrams shown in Fig. 13.

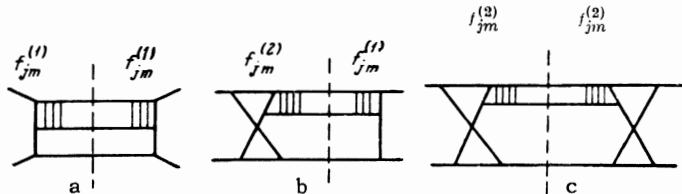


FIG. 13

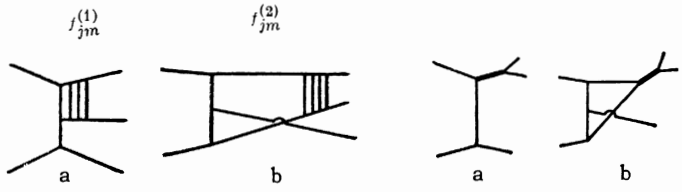


FIG. 14

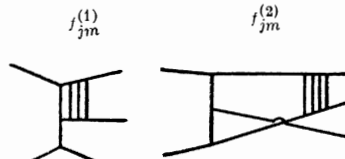


FIG. 15

The amplitudes  $f_{jm}^{(1)}$  and  $f_{jm}^{(2)}$ , which enter in the diagram of Fig. 13, are shown in Figs. 14a and b. For the diagram of Fig. 14a, the continuation of the pair unitarity condition to complex  $j$  does not require introduction of a signature, but for Fig. 14b the signature is essential. This follows from the fact that the unitarity condition for the diagram of Fig. 14b has the usual form for small values of  $s_{13}$  when, as shown above, even continuation of the simplest two-pole diagram calls for introduction of a

signature. For the diagram of Fig. 14a, we begin with the unitarity condition in the region of small  $s_{12}$ , where no signature is required for a continuation of the simplest two-pole diagram. It is clear that the continuation of the amplitudes  $f_{jm}^{(1)}$  and  $f_{jm}^{(2)}$  themselves, which are determined by the pair unitarity conditions, also calls for introduction of a signature in the case of Fig. 14b and not in the case of 14a. Consequently,  $\varphi_{jj+n}^{(1)} = 0$  and  $\varphi_{jj+n}^{(2)} \neq 0$ .

This result is natural if we regard the reggeons as particles, for in this case the diagrams of Fig. 14 are transformed into the diagrams of Fig. 15. It is clear that the diagram of Fig. 15a has one cut in the momentum transfer and therefore requires no signature; the diagram of Fig. 15b contains two cuts (by virtue of the presence of a third spectral function), and therefore is continued to complex  $j$  with signature. Thus, there should be no branch points in the diagrams of Figs. 13a and b, but they should appear in the diagram of Fig. 13c, in accordance with the results of Mandelstam<sup>[1]</sup> and Wilkin<sup>[6]</sup>.

## 5. THREE-PARTICLE CONTRIBUTION TO THE UNITARITY CONDITION FOR THE SCATTERING AMPLITUDES

In the introduction to this paper we wrote out the three-particle contribution to the unitarity condition for the partial amplitude of elastic scattering in the case of complex  $j$ . This unitarity condition was used earlier<sup>[3]</sup> to explain the occurrence of Mandelstam branch points. In<sup>[3]</sup> we did not consider questions connected with the concrete character of the continuation of the amplitudes  $f_{jm}$  and  $\varphi_{jj+n}$ . We likewise did not investigate the possible change in the region of integration for complex  $j$ , nor did we prove the decrease of the three-particle contribution for large values of  $\text{Re } j$ . In addition, we did not discuss the difficulties connected with the convergence properties of the infinite sums in  $m$  and  $n$ , contained in (1). In this article we disregard, as before, questions of summation with respect to  $m$  and  $n$  and confine ourselves to a study of the unitarity condition for the diagrams shown in Fig. 16.

The unitarity condition for the diagram of Fig.

16a is written for complex  $j$  in a perfectly trivial manner

$$\begin{aligned} \frac{1}{2i} [f_j(s) - f_j^*(s)] &= \frac{1}{8(2\pi)^3} \int_{(m_1+m_2)^2}^{\infty} \frac{q_{12}}{\sqrt{s_{12}}} ds_{12} \frac{p_3}{\sqrt{s}} \int_{-1}^{+1} \frac{dx}{2} \\ &\times \frac{1}{2p_3 p_5} Q_j(z_{30}) - \frac{1}{2p_3 p_7} Q_j(z_{30}'). \end{aligned} \quad (30)$$

It is easy to see that the right side of (30) decreases with  $j$ , since  $z_{30}$  and  $z'_{30}$  are larger than unity in the entire region of integration. The continuation (30) is, of course, the only decreasing continuation. Thus, for the diagram of Fig. 16a, the region of integration with respect to  $s_{12}$  and  $x$  is the same as in the case of integer  $j$ . This is perfectly natural, inasmuch as in (30) the singularities of the integrand do not approach the contour of integration with respect to  $x$  for any values of  $s_{12}$ . The only singularity of the integrand is here the line  $p_3 = 0$  on the Dalitz plane, which is attained only on the edge of integration with respect to  $s_{12}$ .

If we proceed somewhat differently and integrate first with respect to the angle between  $\mathbf{p}_2$  and  $\mathbf{q}_{13}$ , fixing, for example,  $s_{13}$ , then a singularity (the line  $p_3 = 0$ ) approaches and overtakes the integration contour. Unlike the cases considered in the preceding section, we can easily show that here the value of  $s_{13}$  at which the contour is overtaken is a singularity of the integral with respect to the angle. There is therefore nothing surprising in the fact that the overtaken sections of the contour lead to an increase with respect to  $j$  in the unitarity condition. (The presence of the increase is obvious, in view of the singularity of the decreasing continuation (30).)

We now proceed to the diagram of Fig. 16b. We write first the unitarity condition, and then explain its derivation:

$$\begin{aligned} \frac{1}{2i} [f_j(s) - f_j^*(s)] &= \frac{1}{8(2\pi)^3} \int_{(m_1+m_2)^2}^{\infty} \frac{q_{12}}{\sqrt{s_{12}}} \frac{p_3}{\sqrt{s}} ds_{12} \\ &\times \left\{ \int_{-1}^{+1} \frac{dx}{2} \left[ \frac{1}{2p_3 p_5} Q_j(z_{30}) \right] \left[ \frac{1}{2p_1 p_6} P_j(-z_{13}) Q_j(z_{10}') \right] \right. \\ &- \frac{2}{\pi} \theta(s_{12} - s_{12}^{(0)}) \sin \pi j \int_1^{x_1} \frac{dx}{2} \frac{1}{2p_3 p_5} Q_j(z_{30}) \frac{1}{2p_1 p_6} \\ &\left. \times Q_j(z_{13}) Q_j(z_{10}') \right\}. \end{aligned} \quad (31)$$

The first of the integrals with respect to  $x$  is the usual integral in the unitarity condition for the diagram of Fig. 16b at integer  $j$ . At complex  $j$ , the integrand function increases sufficiently slowly

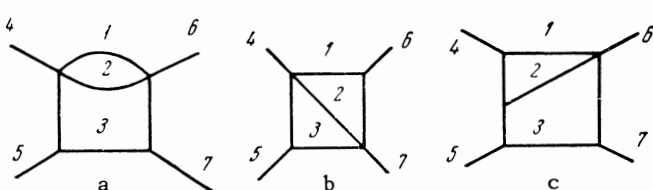


FIG. 16

when  $s_{12}$  is small. If we first integrate with respect to  $x$  for fixed small  $s_{12}$ , and then increase  $s_{12}$  then, when  $s_{12} = s_{12}^{(1)}$ , the singularity  $x_1^-(s_{12})$  (the line  $p_1 = 0$ ) overtakes the integration contour. The second integral in (31) is precisely the result of integration over the overtaken section of the contour. We shall now prove that the continuation (31) is correct; in view of the absence of a signature, it is sufficient to prove here that the right side of (31) increases more slowly than  $\exp(\pi|\operatorname{Im} j|)$ .

Let us consider the expression in the curly brackets in (31) for different  $s_{12}$ . When  $s_{12} < s_{12}^{(1)}$  it can be easily seen that it increases more slowly than  $\exp(\pi|\operatorname{Im} j|/2)$ . When  $s_{12} > s_{12}^{(1)}$ , this expression can be rewritten in the form

$$\{\dots\} = \frac{1}{2\pi i} \int_C dx \frac{1}{4p_1 p_3 p_5 p_6} Q_j(z_{30}) Q_j(-z_{13}) Q_j(z_{10'}), \quad (32)$$

where the contour  $C$  is shown in Fig. 17. It is easy to verify that even for a small deformation of the contour away from the real axis the integrand in (32) increases everywhere on the contour more slowly than  $\exp(\pi|\operatorname{Im} j|)$ . A special situation arises when  $s_{12}$  tends to the upper limit  $(\sqrt{s} - m_3)^2$  ( $p_3 \rightarrow 0$ ). Then the point  $x_1^{-1}$  goes off to  $+\infty$  and the integral with respect to  $x$  could start increasing like  $\exp(\pi|\operatorname{Im} j|)$ . However, owing to the presence of the factor  $Q_j(z_{30}) \sim p_3^{j+1}$ , the entire integral (32) tends to zero at small  $p_3$ . Thus, the entire right side of (31) increases more slowly than  $\exp(\pi|\operatorname{Im} j|)$ . On the other hand, since the Mandelstam representation for the diagram of Fig. 16b has been proved (see [7]), and with it the existence of a non-growing continuation, the continuation (31) does not grow at all, by virtue of the uniqueness.

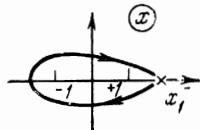


FIG. 17

From the symmetry of the diagram of Fig. 16b it is obvious that everything stated above concerning the unitarity condition (31) remains in force if we start the integration with respect to the angle at small fixed values of  $s_{23}$ . On the other hand, if we start the integration with respect to the angle between  $p_2$  and  $q_{23}$  at constant  $s_{13}$ , then two encounters with the lines  $p_1 = 0$  and  $p_3 = 0$  take place. These encounters, as before, lead to singularities in  $s_{13}$ , and when  $s_{13}$  is lower than the upper limit of integration  $(\sqrt{s} - m_2)^2$ , the integral

with respect to the angle grows more slowly than  $\exp(\pi|\operatorname{Im} j|)$ . However, when  $s_{13} = (\sqrt{s} - m_2)^2$  the integral does not vanish, and increases like  $\exp(\pi|\operatorname{Im} j|)$ . Therefore the continuation of the unitarity condition which is obtained thereby is incorrect. The unitarity conditions (30) and (31) for the diagrams of Figs. 16a and b are analogous to the unitarity conditions obtained in the nonrelativistic model [8]. For the diagram of Fig. 16c we shall not write out explicitly the unitarity condition at complex  $j$ , since it is analogous to the case of the diagram of Fig. 16b. Here, however, it is permissible to integrate only with respect to  $x$ , starting the integration initially with small  $s_{12}$ . As in the case of the diagram of 16b, when  $s_{12}$  increases the contour of integration with respect to  $x$  is overtaken by the singularity  $x_1^-$ .

## APPENDIX 1

Let us find an expression for some of the quantities characterizing the three-particle system, in terms of  $s_2$  and  $x$ . We deal with two coordinate systems: 1) the system of the common center of mass and 2) the center of mass system of particles 1 and 2. It is obvious that the second system moves relative to the first with velocity  $v = -p_3/(E - E_3)$  ( $\sqrt{s} = E = E_1 + E_2 + E_3$ ,  $E_i$ —particle energy in the common c.m.s.). The Lorentz transformation corresponding to this velocity, as applied to the momentum of particle 1, yields ( $q_{12}$  is the momentum of particle 1 in the c.m.s. of particles 1 and 2):

$$p_1(1 - z_{13}^2)^{1/2} = q_{12}(1 - x^2)^{1/2}, \\ p_1 z_{13} = \left( q_{12}x - \frac{p_3}{E - E_3} \epsilon_1 \right) \frac{E - E_3}{\sqrt{s_{12}}} \quad (A.1)$$

where the first equation relates the transverse and the second the longitudinal components of the momentum  $p_1$  in the two coordinate frames. From (A.1) we can easily obtain expressions for  $p_1$  and  $z_{13}$ :

$$p_2^2 = \frac{q_{12}^2 p_3^2}{s_{12}} (x - x_1^+) (x - x_1^-), \quad (A.2)$$

$$z_{13} = \left( \frac{E - E_3}{p} x - \frac{\epsilon_1}{q_{12}} \right) [(x - x_1^+) (x - x_1^-)]^{-1/2}, \quad (A.3)$$

$$x_1^\pm = \frac{E - E_3}{p_3} \frac{\epsilon_1}{q_{12}} + \frac{\sqrt{s_{12}} m_1}{p_3 q_{12}} \quad (A.4)$$

We can analogously derive the formulas

$$p_2^2 = \frac{q_{12}^2 p_3^2}{s} (x + x_2^+) (x + x_2^-),$$

$$z_{23} = \left( -\frac{E - E_3}{p_3} x - \frac{\epsilon_2}{q_{12}} \right) [(x + x_2^+) (x + x_2^-)]^{-1/2},$$

$$z_{12} = \left( -x^2 + x \frac{E - E_3}{p_3 q} (\varepsilon_1 - \varepsilon_2) + \frac{\varepsilon_1 \varepsilon_2}{q^2} - \frac{s_{12}}{p^2} \right) \\ \times [(x - x_1^+) (x - x_1^-) (x + x_2^+) (x + x_2^-)]^{-1/2}, \quad (A.5)$$

$$x_2^\pm = \frac{E - E_3}{p_3} \frac{\varepsilon_2}{q_{12}} + \frac{\sqrt{s_{12}}}{p_3} \frac{m_2}{q_{12}} \quad (A.6)$$

In addition

$$E_3 = (s - s_{12} + m_3^2) / 2\sqrt{s} = (p_3^2 + m_3^2)^{1/2}, \\ \varepsilon_1 = (s_{12} + m_1^2 - m_2^2) / 2\sqrt{s_{12}} = (q_{12}^2 + m_1^2)^{1/2}, \\ \varepsilon_2 = (s_{12} + m_2^2 - m_1^2) / 2\sqrt{s_{12}} = (q_{12}^2 + m_2^2)^{1/2}. \quad (A.7)$$

Finally, the following obvious relations between the cosines  $z_{12}$ ,  $z_{13}$ , and  $z_{23}$  are useful:

$$z_{12} = z_{13} z_{23} - [(1 - z_{13}^2)(1 - z_{23}^2)]^{1/2}, \\ (1 - z_{12}^2)^{1/2} = -z_{23}(1 - z_{13}^2)^{1/2} - z_{13}(1 - z_{23}^2)^{1/2}. \quad (A.8)$$

## APPENDIX 2

To calculate the addition to the unitarity condition (24), let us consider values of  $s_{12}$  larger than  $s_{12}^{(1)}$ , when the encounter with the contour with respect to  $x'$  has already taken place. When  $x' < 1$ , the function  $f_{jm}^{(0)}$  is given by (26), where the contour integrals with respect to  $z$  grow from the complex-conjugate branch points (Fig. 5):

$$z^{(\pm)} = -z_{13} z_{10} \pm i[(1 - z_{13}^2)(z_{10}^2 - 1)]^{1/2}. \quad (A.9)$$

When  $x' = 1$  ( $z_{13} = +1$ ), the singularities  $z^{(\pm)}$  fall on the real axis at the point  $z = -z_{10}$ . They turn out to be on opposite sides of the cut  $Q_{jm}(z)$ , which travels from  $z = +1$  to  $-\infty$ . If we continue to increase  $x'$ , then the singularities move on the real axis—one to the right and the other to the left. After circling the point  $x' = 1$  from above, as shown in Fig. 10, the arrangement of the integration contours in the  $z$  plane, determining  $f_{jm}^{(0)+}$  in formula (27), is that shown in Fig. 18. Figure 18 shows also the phases of the root  $K^{1/2}(z, z_{10} - z_{13})$  in the integral (26). When going around the point  $x_1^-$  ( $p_1 = 0$ ) clockwise (Fig. 10), the singularity  $z^{(-)}$  goes off to  $-\infty$ , moves counterclockwise along a large circle, and falls on the upper edge of the cut  $Q_{jm}(z)$ . The point  $z^{(+)}$  remains immobile.

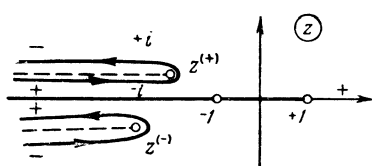


FIG. 18

The new arrangement of the contours, which now determine  $f_m^{(0)-}$ , is shown in Fig. 19. The figure shows also the new phases of  $K^{1/2}(z, z_{10}, -z_{13})$ . As

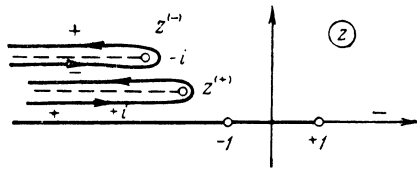


FIG. 19

easily seen from Fig. 19, only the integration with respect to  $z$  between the points  $z^{(-)}$  and  $z^{(+)}$  remains in  $f_{jm}^{(0)-}$ . By calculating now the difference  $f_{jm}^{(0)+} - f_{jm}^{(0)-}$  (it is necessary here to take into account the additional change in sign due to the factor  $1/p_1$  in formula (26)), and recognizing that

$$1/2i[Q_{jm}(z + ie) - Q_{jm}(z - ie)] = \sin \pi j Q_{jm}(-z) (z < -1),$$

we arrive at expression (27). It is easily seen that the result does not depend on the manner in which the singularity  $x_1^-$  goes around the point  $x' = 1$  (this corresponds to different manners of going around the point  $s_{12} = s_{12}^{(0)}$ ). This is seen from the fact that the obtained addition (27) is real.

## APPENDIX 3

Let us consider expression (27) for the addition to the unitarity condition. The function  $f_m$  has root branch points with respect to  $x'$  at  $x' = \xi x \pm [(\xi^2 - 1)(x^2 - 1)]^{1/2}$ . When  $x^2 < 1$ , these singularities are complex, and when  $x = 1$  they go on the real axis, moving further along it in opposite directions. From formula (A.4) we see that with increasing  $s_{12}$ , when  $p_3 \rightarrow 0$ , the upper limit of integration in (27) becomes  $x_1^- \rightarrow +\infty$ . On the other hand, the singularities  $\xi x \pm [(\xi^2 - 1)(x^2 - 1)]^{1/2}$  remain finite. Therefore when  $x \geq 1$  there is always some physical value of  $s_{12}$  at which  $x_1^-$  coincides with either of the points  $\xi x \pm [(\xi^2 - 1)(x^2 - 1)]^{1/2}$ . These values of  $s_{12}$  (which depend on  $x$ ) are singular for the diagram in Fig. 8b. The singularities obtained do not fall inside the physical region, where  $x^2 < 1$ , but touch its boundary ( $x = 1$ ) at some value of  $s_{12}$ .

## APPENDIX 4

The amplitude  $f_{jm}^{(0)}$ , which enters in formula (28), has the following form (see formula (13)):

$$f_{jm}^{(0)} = \frac{1}{2\pi i} \frac{1}{4p_1 p_3 p_4 p_5} \left\{ \pm \int_{(14a)} dz Q_{jm}(-z) (z^2 - 1)^{m/2} \right. \\ \times \frac{1}{z_0 - z} \left[ \frac{1 - z_{23}^2}{1 - z_{13}^2} \right]^{1/2} \\ \times \left. \frac{1}{K^{1/2}(z, z_{30}, z_{23})} \left[ \frac{z_{30} - z_{23}z + K^{1/2}(z, z_{30}, z_{23})}{(1 - z_{23}^2)^{1/2}} \right]^{-m} \right\}$$

$$\begin{aligned}
& + \int_{(14b)} dz Q_{jm}(z) (z^2 - 1)^{m/2} \frac{1}{z_0 - z} \times \left[ \frac{1 - z_{12}^2}{1 - z_{13}^2} \right]^{1/2} \\
& \times \frac{1}{K^{1/2}(z, z_{10}, -z_{12})} \left[ \frac{z_{10} + z_{12}z + K^{1/2}(z, z_{10}, -z_{12})}{(1 - z_{12}^2)^{1/2}} \right]^{-m}.
\end{aligned} \quad (A.10)$$

$z_0$  is given here by (17); the integrations with respect to  $z$  are carried out over contours which enclose the cuts from the singularities (14a) and (14b);  $(z^2 - 1)^{1/2} > 0$  when  $z > 0$ . The plus (minus) sign in front of the first integral corresponds to positive (negative) signature in  $j$ .

Continuing expressions (28) and (A.10) with respect to  $s_{13}$ , in analogy with the diagram of Fig. 8b, we observe that when  $s_{13} = s_{13}^{(1)}$  and  $s_{13} = s_{13}^{(3)}$  (Fig. 12) the contour of integration with respect to  $x'$  is overtaken by the singularities connected with the lines  $p_1 = 0$  and  $p_3 = 0$ . Unlike the diagram of Fig. 8b, both ends of the integration contour with respect to  $x'$  are now overtaken, so that when  $s_{13} > s_{13}^{(1)}$ ,  $s_{13}^{(3)}$  the integration on the Dalitz plane is carried out between the lines  $p_1 = 0$  and  $p_3 = 0$ . Let us write out in explicit form the resultant addition to the unitarity condition, (28). It is calculated in a manner similar to that given in Appendix 2:

$$\Delta = \Delta_1 + \Delta_3;$$

$$\begin{aligned}
\Delta_1 = & \theta(s_{13} - s_{13}^{(1)}) \sin \pi j \frac{q_{13}}{8\pi \sqrt{s_{13}}} \int_{-1}^{\xi_1^-} \frac{dx'}{2} \left\{ \frac{1}{2q_{13}^2} \frac{1}{K^{1/2}(\zeta, x, x')} \right. \\
& \times \left. \left[ \frac{\zeta - xx' + K^{1/2}(\zeta, x, x')}{[(1 - x^2)(x'^2 - 1)]^{1/2}} \right]^{-m} \right\} \frac{1}{4p_1 p_3 p_4 p_5} \\
& \times \frac{1}{\pi} \int_{L_1} dz Q_{jm}(z) (z^2 - 1)^{m/2} \frac{1}{z_0 + z} \left[ \frac{z_{12}^2 - 1}{z_{13}^2 - 1} \right]^{1/2} \\
& \times \frac{1}{K^{1/2}(z, z_{10}, z_{12})} \left[ \frac{z_{10} - z z_{12} + K^{1/2}(z, z_{10}, z_{12})}{(z_{12}^2 - 1)^{1/2}} \right]^{-m},
\end{aligned} \quad (A.11)$$

$$\begin{aligned}
\Delta_3 = & \pm \theta(s_{13} - s_{13}^{(3)}) \sin \pi j \frac{q_{13}}{8\pi \sqrt{s_{13}}} \int_{-\xi_1^-}^{-1} \frac{dx'}{2} \\
& \times \left\{ \frac{1}{2q_{13}^2} \frac{1}{K^{1/2}(\zeta, x, x')} \left[ \frac{\zeta - xx' + K^{1/2}(\zeta, x, x')}{[(1 - x^2)(x'^2 - 1)]^{1/2}} \right]^{-m} \right\} \\
& \times \frac{(-1)^{m+1}}{4p_1 p_3 p_4 p_5} \int_{L_3} dz Q_{jm}(z) (z^2 - 1)^{m/2} \frac{1}{z_0 - z} \\
& \times \left[ \frac{z_{23}^2 - 1}{z_{13}^2 - 1} \right]^{1/2} \\
& \times \frac{1}{K^{1/2}(z, z_{30}, z_{23})} \left[ \frac{z_{30} - z_{23}z + K^{1/2}(z, z_{30}, z_{23})}{(z_{23}^2 - 1)^{1/2}} \right]^{-m}; \quad (A.12)
\end{aligned}$$

$$\xi_1^- = \frac{(p_2^2 + s_{13})^{1/2}}{p_2} \frac{(q_{13}^2 + m_1^2)^{1/2}}{q_{13}} - \frac{\sqrt{s_{13}}}{p_2} \frac{m_1}{q_{13}}$$

$$\xi_3^- = \frac{(p_2^2 + s_{13})^{1/2}}{p_2} \frac{(q_{13}^2 + m_3^2)^{1/2}}{q_{13}} - \frac{\sqrt{s_{13}}}{p_2} \frac{m_3}{q_{13}}. \quad (A.13)$$

In formulas (A.11) and (A.12) the contours  $L_1$  and  $L_3$  overtake respectively the cuts  $K^{1/2}(z, z_{10}, z_{12})$  and  $K^{1/2}(z, z_{30}, z_{23})$ , which go from the points  $z_{12}z_{10} + [(z_{10}^2 - 1)(z_{12}^2 - 1)]^{1/2}$  and  $z_{23}z_{30} + [(z_{30}^2 + 1)(z_{23}^2 - 1)]^{1/2}$ : the integration is carried out in such a way that the starts of the cuts are circuited clockwise.

As mentioned in the text, the amplitude  $f_{jm}^{(0)}(s_{13}, x')$  has one more singularity, the trajectory of which is represented by the curve  $K$  in Fig. 12. The equation for this curve is determined by the condition that the pole  $z = z_0$  coincide with the zeroes  $K(z, z_{10}, -z_{12})$  and  $K(z, z_{30}, z_{23})$ . If  $z = z_0$ , then  $K(z, z_{10}, -z_{12})$  and  $K(z, z_{30}, z_{23})$  are equal to  $K(z_{10}, z_{30}, -z_{13})$ , apart from a factor which is of no importance to us.

The equation

$$K(z_{10}, z_{30}, -z_{13}) = 0 \quad (A.14)$$

determines therefore the curve  $K$ :  $x = x_K(s_{13})$ . When  $z_{13} = -1$  (the limit of the physical region), (A.14) reduces to the equality  $z_{10} = z_{30}$ . This equality determines the value of  $s_{13}^{(0)}$  at which the curve  $K$  is tangent to the circle (point A on Fig. 12). It is easy to show that this point always lies at physical values of the pair energy, and that  $s_{13}^{(0)} > s_{13}^{(1)}$ . When  $s_{13} < s_{13}^{(0)}$ , the singularity  $K$  does not change the form of the unitarity condition, since it is not contained in the discontinuities of  $f_{jm}^{(0)}(s_{13}, x')$  on the singularities of (A.13).

When  $s_{13} > s_{13}^{(0)}$ , this singularity links with the main contour of integration with respect to  $x'$ , which goes from  $-1$  to  $+1$ .

Direct calculation for the addition to the unitarity condition (28) shows that when  $s_{13} > s_{13}^{(0)}$  the addition can be written in the form

$$\Delta = \Delta'_1 + \Delta_3 + \Delta_0. \quad (A.15)$$

Here  $\Delta'_1$  is determined by (A.11), in which the integration with respect to  $z$  is taken in the sense of the principal value, and

$$\begin{aligned}
\Delta_0 = & \theta(s_{13} - s_{13}^{(0)}) (-\cos \pi j \pm 1) \frac{q_{13}}{8\pi \sqrt{s_{13}}} \\
& \times \int_{-1}^{x_K(s_{13})} \frac{dx'}{2} \left\{ \frac{1}{2q_{13}^2} \frac{1}{\sqrt{K(\zeta, x, x')}} \right. \\
& \times \left. \left[ \frac{\zeta - xx' + K^{1/2}(\zeta, x, x')}{[(1 - x^2)(x'^2 - 1)]^{1/2}} \right]^{-m} \right\} \frac{1}{4p_1 p_3 p_4 p_5} \\
& \times Q_{jm}(-z_0) (z_0^2 - 1)^{m/2}
\end{aligned}$$

$$\begin{aligned} & \times \left[ \frac{z_{12}^2 - 1}{z_{13}^2 - 1} \right]^{1/2} \frac{1}{K^{1/2}(-z_0, z_{10}, z_{12})} \\ & \times \left\{ \left[ \frac{z_{10} + z_0 z_{12} + K^{1/2}(-z_0, z_{10}, z_{12})}{(z_{12}^2 - 1)^{1/2}} \right]^{-m} \right. \\ & \left. + \left[ \frac{z_{10} + z_0 z_{12} - K^{1/2}(-z_0, z_{10}, z_{12})}{(z_{12}^2 - 1)^{1/2}} \right]^{-m} \right\}. \quad (\text{A.16}) \end{aligned}$$

The  $\pm$  sign is determined by the signature with respect to  $j$ .

Our calculations correspond to the case shown in Fig. 12, when we have  $x = +1$ ,  $z_{12} = +1$ , and  $z_{23} = -1$  at the point of tangency A, so that  $z_0 < -1$ . Were this point to lie on the other half of the circle, then  $z_0$  would be larger than unity. The expression for the addition would in this case have a somewhat different form.

<sup>1</sup>S. Mandelstam, Nuovo cimento **30**, 1148 (1963).

<sup>2</sup>Gribov, Pomeranchuk, and Ter-Martirosyan, ITEF Preprint, 1964.

<sup>3</sup>Azimov, Ansel'm, Gribov, Danilov, and Dyatlov, JETP **48**, 1776 (1965), Soviet Phys. JETP **21**, 1189 (1965).

<sup>4</sup>N. N. Meiman, Lecture in the collection Voprosy teorii elementarnykh chasit (Problems of Elementary Particle Physics), Erevan, 1962.

<sup>5</sup>M. Jacob and G. C. Wick, Ann. of Phys. **7**, 404 (1959).

<sup>6</sup>C. Wilkin, Nuovo Cimento **31**, 377 (1963).

<sup>7</sup>V. N. Gribov and I. T. Dyatlov, JETP **42**, 196 (1962), Soviet Phys. JETP **15**, 140 (1962).

<sup>8</sup>Azimov, Gribov, Danilov, and Dyatlov, YaF **1**, 1121 (1965), Soviet JNP **1**, 798 (1965).

Translated by J. G. Adashko  
74